GENETICS

A far-red light–inducible CRISPR-Cas12a platform for remote-controlled genome editing and gene activation

Xinyi Wang[1], Kaili Dong[1], Deqiang Kong[1], Yang Zhou[1], Jianli Yin[1], Fengfeng Cai[2], Meiyan Wang[1]*, Haifeng Ye[1]*

Copyright © 2021 The Authors, some rights reserved; exclusive licensee American Association for the Advancement of Science. No claim to original U.S. Government Works. Distributed under a Creative Commons Attribution NonCommercial License 4.0 (CC BY-NC).

The CRISPR-Cas12a has been harnessed as a powerful tool for manipulating targeted gene expression. The possibility to manipulate the activity of CRISPR-Cas12a with a more precise spatiotemporal resolution and deep tissue permeability will enable targeted genome engineering and deepen our understanding of the gene functions underlying complex cellular behaviors. However, currently available inducible CRISPR-Cas12a systems are limited by diffusion, cytotoxicity, and poor tissue permeability. Here, we developed a far-red light (FRL)–inducible CRISPR-Cas12a (FICA) system that can robustly induce gene editing in mammalian cells, and an FRL-inducible CRISPR-dCas12a (FIdCA) system based on the protein-tagging system SUperNova (SunTag) that can be used for gene activation under light-emitting diode–based FRL. Moreover, we show that the FIdCA system can be deployed to activate target genes in mouse livers. These results demonstrate that these systems developed here provide robust and efficient platforms for programmable genome manipulation in a noninvasive and spatiotemporal fashion.

INTRODUCTION

CRISPR systems have been harnessed for the manipulation of genes of interest in a variety of organisms (*1*–*8*). CRISPR-Cas12a (Cpf1) is another member of the class II type V CRISPR-Cas system that has expanded the gene editing toolbox because of its unique RNA processing features (*9*–*15*). Cas12a is a smaller endonuclease than Cas9, can be easily packaged for delivery, and functions both as a deoxyribonuclease and a ribonuclease that can process multiple shorter CRISPR RNAs (crRNAs) from a single transcript (*16*). Cas12a is able to recognize a T-rich protospacer-adjacent motif (PAM) and generate a staggered cut with a 5′ overhang that facilitated nonhomologous end joining (NHEJ)–based gene insertion into the mammalian genome (*9*), while the T-rich PAM of Cas12a is an ideal complement to the G-rich PAM of Cas9 (*17*–*20*). Furthermore, Cas12a has higher binding sequence specificity to the target DNA and lower off-target effects than Cas9 (*19*, *21*, *22*). The most commonly used Cas12a originates from *Acidaminococcus* sp. (AsCas12a) and *Lachnospiraceae bacterium* (LbCas12a). Both of these Cas12a molecules exhibit a comparable CRISPR-Cas9 genome editing efficiency in prokaryotes and eukaryotes (*23*–*26*), and recent studies showed that they could be used for genome editing in mammalian cells (*25*, *27*). Moreover, the nuclease-dead Cas12a (dCas12a) could be used in the regulation of endogenous and exogenous gene expression in human cells (*28*, *29*). However, only a few regulated CRISPR-Cas12a systems have been reported. This contrasts with the Cas9 systems, which have been engineered to dynamically regulate gene expression using chemical (*30*, *31*), ultrasonic (*32*), temperature (*33*), and light (*34*–*37*) stimuli. This disparity might result from different Cas12a and Cas9 structures, making it difficult to develop modified Cas12a in a similar manner to Cas9 engineering. Regardless, it is still necessary to develop technologies for controlling Cas12a systems in an orthogonal and inducible manner.

Recently, two chemical-inducible dCas12a systems have been developed to activate or repress the transcription of endogenous genes in response to external ligands (*38*) and rapamycin (*23*). However, it is difficult to remove chemical inducers from the system, and rapamycin may also induce adverse effects by perturbing the endogenous mammalian target of rapamycin mTOR pathway (*39*). In contrast, light is an ideal inducer for establishing a noninvasive, spatiotemporal control of gene expression (*40*–*42*). Recently, a blue light–controlled split-LbCpf1 system was developed to control genome editing in a tunable manner by using the Magnet-based Cpf1 system (*43*). However, the high energy of blue light leads to relatively strong phototoxic effects on mammalian cells and an insufficient penetrative capability in vivo (*44*). These properties severely restrict the use of blue light–based optogenetic devices for downstream in vivo translational research and clinical applications.

To address these limitations, we sought to develop an inducible far-red light (FRL)–responsive Cas12a system to achieve controllable genome/epigenome engineering with low phototoxicity and background activity that can be fine-tuned for diverse applications. The longer wavelength and deep tissue penetration of red/FRL led us to engineer an FRL-inducible CRISPR-Cas12a (FICA) system and an FRL-inducible CRISPR-dCas12a (FIdCA) system based on the bacterial phytochrome BphS optical controllable system that was previously established by our group (*45*). This strategy ensured little cytotoxicity and deep tissue penetration capacity (*45*, *46*), and our previous FRL-activated split-Cas9/dCas9 systems (FAST/FACE) have been demonstrated to opto-control genome editing and gene activation with spatiotemporal resolution (*36*, *37*). Thus, in this study, we started by assembling the FICA system components in mammalian cells and, using light-emitting diode (LED)–based FRL, demonstrate the successful activation of targeted genome editing, which showed more efficient FRL-inducible genome editing compared

[1]Synthetic Biology and Biomedical Engineering Laboratory, Biomedical Synthetic Biology Research Center, Shanghai Key Laboratory of Regulatory Biology, Institute of Biomedical Sciences and School of Life Sciences, East China Normal University, Dongchuan Road 500, Shanghai 200241, China. [2]Department of Breast Surgery, Yangpu Hospital, School of Medicine, Tongji University, 450 Tengyue Road, Shanghai 200090, China.
*Corresponding author. Email: mywang@bio.ecnu.edu.cn (M.W.); hfye@bio.ecnu.edu.cn (H.Y.)

Downloaded from https://www.science.org at Shanghai Normal University on December 16, 2021

with FAST system for selected genomic loci. Subsequently, we demonstrated that the assembled FIdCA system enabled transcriptional activation of user-defined exogenous or endogenous genes under FRL, which has the potential to activate endogenous human genes with greater efficiency compared with FACE. Moreover, the FIdCA system successfully controlled transgene expression in mouse livers by FRL. Our study illustrates a promising FICA platform for precise gene regulation with high spatiotemporal resolution.

RESULTS

Construction of a FICA system

To develop an improved optogenetically controlled Cas12a system with deep tissue penetrative capacity and low phototoxicity, we constructed a FICA system using our previously reported bacteriophytochrome-based optogenetic system without exogenous supplement of biliverdin; this should be possible, as the endogenous BV present in mammalian cells is known to be sufficient to activate BphS (*44*, *45*). In this system, the FRL activated bacterial photoreceptor BphS converts guanosine triphosphate (GTP) into cyclic diguanylate monophosphate (c-di-GMP) (*47*), and subsequently, c-di-GMP triggers the dimerization of the hybrid transactivator BldD-p65-VP64 (*48*) (BldD; a c-di-GMP–binding domain derived from sporulating actinomycete bacteria), which further translocates into the nucleus and binds to its cognitive synthetic promoter P_{FRL} (*45*). Besides, the c-di-GMP phosphodiesterase YhjH is coexpressed to reduce basal intracellular c-di-GMP production (*47*) that enables robust FRL-triggered Cas12a expression (Fig. 1A). Then, the Cas12a-crRNA complexes efficiently cleave the target DNA sequence to generate gene deletions and insertions (fig. S1). We first tested whether FRL could control Cas12a expression by fusing enhanced green fluorescent protein (EGFP) to the C terminus of Cas12a. We found that FRL LED substantially increased EGFP expression (10.8-fold) when compared with control cells incubated in the dark, which demonstrated that FRL successfully induced Cas12a expression (Fig. 1, B and C). We next assessed the FICA-mediated gene editing activity in human embryonic kidney 293T (HEK-293T) cells using destabilized enhanced yellow fluorescent protein (d2EYFP) as a reporter. After cotransfecting cells with a FICA system iteration comprising the FRL-responsive sensor vector pXY137, the light-inducible Cas12a expression vector pDL192, the *d2EYFP* reporter, and two crRNAs targeting *d2EYFP*, we detected successful editing of the exogenous *d2EYFP* sequence upon FRL (fig. S2).

To test whether the FICA system can cleave targeted endogenous genomic loci and induce indel mutations in an FRL fashion, we delivered the aforementioned FICA system into HEK-293T cells together with a crRNA targeting the human *DNMT1* locus pZQ28 (Fig. 1D). This combination was able to successfully induce indel mutations in the targeted human *DNMT1* locus under FRL using the mismatch-sensitive T7 endonuclease I (T7E1) assay. However, we also observed background indels under dark conditions (fig. S3A). To reduce the background activity, we optimized plasmid ratios of the FICA system and found that the cells that were transfected with pXY137 (125 ng), pDL192 (25 ng), and pZQ28 (100 ng) exhibited an efficient cleavage in the targeted human *DNMT1* locus upon FRL (2 mW/cm^2; 730 nm), while no detectable gene editing was observed in the dark (Fig. 1E and fig. S3B). Moreover, the frequency of FICA-induced indel mutations in the human *DNMT1* locus (12.3%) was comparable to that of human cytomegalovirus promoter (P_{hCMV})–driven Cas12a (11.9%) (Fig. 1E).

To confirm the versatility of the FICA system, we cotransfected our system along with different crRNAs targeting another three human gene loci (*FANCF*, *GRIN2B*, and *CXCR*). The T7E1 assay indicated that our FICA system induced efficient gene editing on all endogenous gene loci under FRL, and the gene editing efficiencies obtained by our system across all targeted loci are similar to those induced by constitutively expressed Cas12a driven by the P_{hCMV} promoter (Fig. 1, F to H). We further confirmed that our FICA system could efficiently cleave different targeted regions of the human *DNMT1*, *GRIN2B*, *FANCF*, and *CXCR* loci using the tracking of indels by decomposition (TIDE) analysis. (Fig. 1, I to L). Moreover, we evaluated the gene editing efficiency of the *DNMT1* locus by deep sequencing. Our results showed that targeted deep sequencing yielded 15.7% indel frequency at the *DNMT1* locus in HEK-293T cells (fig. S4). Collectively, these results demonstrated that the FICA system can be used for the optogenetic control of multiplexed endogenous genome editing in mammalian cells.

Gene editing performance of the FICA system

Having demonstrated that the FICA system successfully achieved photoactivatable regulation of exogenous and endogenous gene editing in mammalian cells, we next investigated the FRL-inducible gene editing kinetics of the FICA system. Accordingly, HEK-293T cells were cotransfected with the FICA system, an exogenous fluorescent reporter *d2EYFP*, and two crRNAs that target reporter *d2EYFP*. The data showed that the efficiency of the indel mutations of the exogenous reporter *d2EYFP* depended on the illumination intensity and time of exposure (Fig. 2, A and B). In addition, the FICA system–mediated efficiency of indel mutations in the endogenous *DNMT1* locus increased as the FRL irradiation time and light intensity increased (Fig. 2, C and D). Both exogenous and endogenous gene editing results demonstrated that the FICA system exhibited good tuning ability.

We next compared the gene editing efficiency between the FICA system and FAST system using different crRNAs or single guide RNAs (sgRNAs). The TIDE results revealed that our FICA system could induce indel mutations at endogenous gene target sites in human cells with higher efficiencies [*IL12A-AS1*: 11.9% (FICA) versus 3.1% (FAST); *PRKCH*: 13.9% (FICA) versus 5.6% (FAST)] (fig. S5). These results suggested that the FICA system exhibited more efficient FRL-inducible genome editing for multiple examined endogenous genes of mammalian cells as compared with the FAST system.

Development of a FIdCA system

In addition to genome editing, Cas12a variants have also been used for activating gene expression by fusing catalytically dead Cas12a (dCas12a) to different transcriptional activation domains (*49*). Developing a potent dCas9 activator demonstrated that gene expression is efficiently induced by three activators: VP64-p65-Rta (VPR), synergistic activation mediator (SAM), and SunTag, which contains a total of 10 copies of the GCN4 peptide recruiting single-chain variable fragment (scFv) antibody fusion effector protein (*50*). Therefore, we initially constructed an FRL-inducible dCas12a system by fusing dCas12a to the tripartite VPR activator, which was induced by the FRL-responsive promoter P_{FRL}. This led to a significant activation of both exogenous human placental secreted alkaline phosphatase (SEAP) reporter and endogenous *HBB* gene expression upon FRL (fig. S6). However, this construction had a strong background under dark conditions and low gene activation upon FRL. Hence,

Downloaded from https://www.science.org at Shanghai Normal University on December 16, 2021

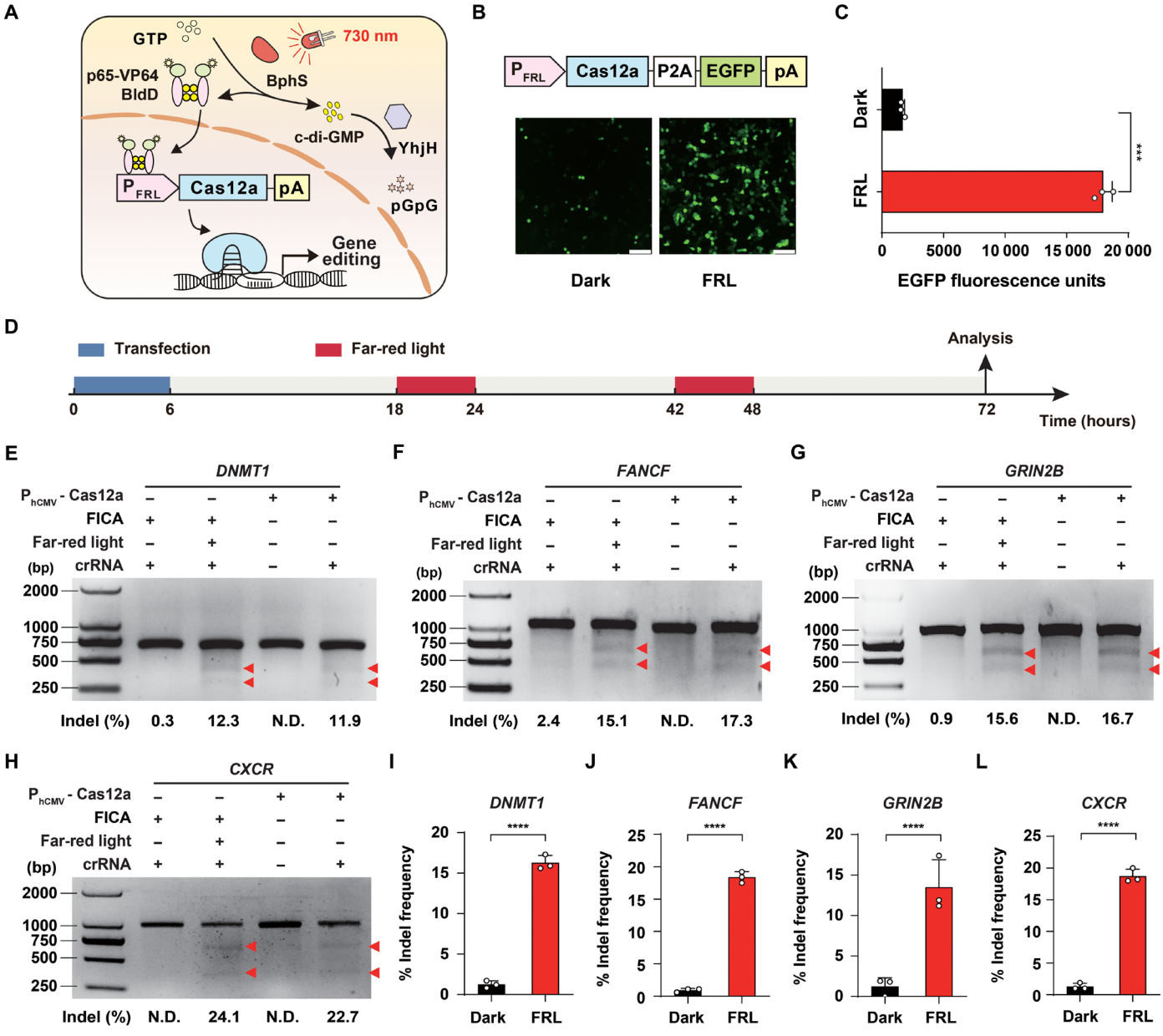


Fig. 1. Development and characterization of a FICA system. (**A**) Schematic representation of the FICA system. FRL (730 nm) irradiation activates the bacterial photoreceptor BphS, which causes GTP conversion into c-di-GMP. In turn, the increase in c-di-GMP induces dimerization of the FRL-dependent transcriptional activator p65-VP64-BldD, which further binds to its synthetic promoter P_{FRL} to initiate the Cas12a expression and exhibit nuclease activity. (**B**) Fluorescence imaging of light-inducible expression of Cas12a-EGFP. Representative images from $n = 3$ biological replicates; scale bars, 100 μm. (**C**) Analysis of light-inducible expression of Cas12a-EGFP by flow cytometry assay. (**D**) Schematic diagram of the time schedule for FICA-mediated genome editing. (**E** to **H**) T7E1 analysis of FICA-mediated gene editing on the human *DNMT1* (E), *FANCF* (F), *GRIN2B* (G), and *CXCR* loci (H). The red arrowheads indicate the expected cleaved products. N.D., not detectable; bp, base pairs. One representative gel image of two individual experiments is shown. (**I** to **L**) Tracking of indels by decomposition (TIDE) analysis of FICA-mediated gene editing on the human *DNMT1* (I), *FANCF* (J), *GRIN2B* (K), and *CXCR* loci (L). Data in (C) and (I) to (L) are expressed as means ± SD; $n = 3$ independent alignment. *P* values were calculated using a Student's *t* test. ***$P < 0.001$ and ****$P < 0.0001$, FRL versus dark. Detailed descriptions of the genetic components and the transfection mixtures are provided in tables S1 and S5.

to increase the gene activation ability upon FRL and reduce the background activity, we engineered an FRL-inducible dCas12a system by the constitutive expression of dCas12a and an FRL-triggered expression of the MCP–p65–HSF1 (MCP: MS2 capsid protein; p65: the 65-kDa transactivator subunit of NF-κB; HSF1: heat shock factor 1) activator, which can be recruited to crRNAs conjugated with MS2 aptamers inserted directly at the top of direct repeat of crRNA (fig. S7A). However, there was no significant *HBB* gene activation (fig. S7B). We hypothesize that this construct disrupted the secondary structure in the stem-loop duplex of the crRNA, which might abolish Cas12a-mediated cleavage. In addition, a previous study had demonstrated that crRNA containing a uridinylate-rich 3′-overhang could improve the

Downloaded from https://www.science.org at Shanghai Normal University on December 16, 2021

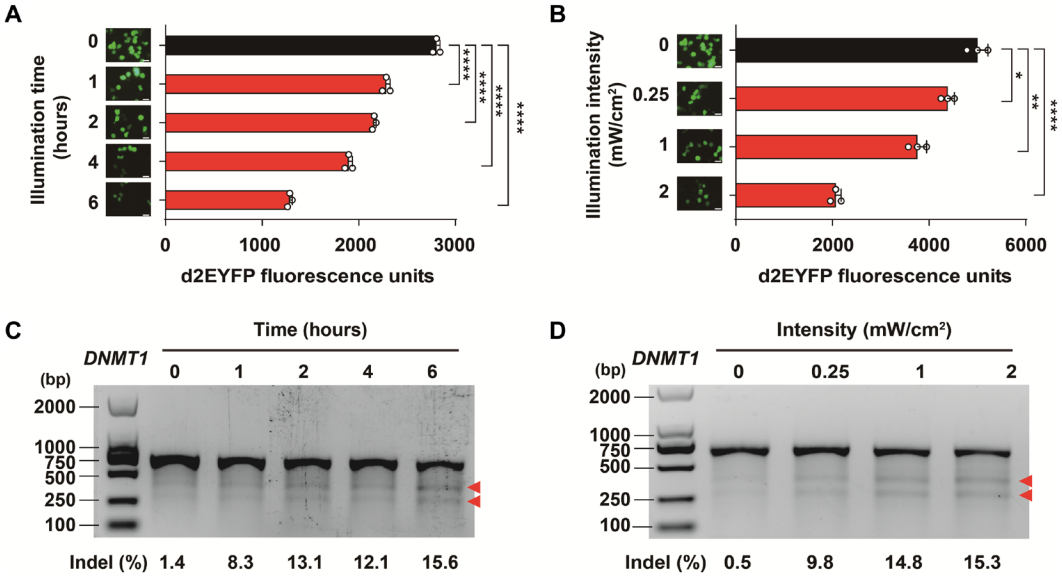


Fig. 2. Characterization of the FICA system. (**A**) Time-dependent FICA-mediated genome editing of the exogenous d2EYFP reporter. Transfected HEK-293T cells were illuminated with FRL (730 nm, 2 mW/cm^2) for different time periods (0 to 6 hours per day) for 2 days; scale bars, 50 μm. The d2EYFP reporter was visualized by fluorescence microscopy and quantified by flow cytometry 48 hours after the first illumination. (**B**) Intensity-dependent FICA-mediated genome editing of the exogenous reporter d2EYFP. Transfected HEK-293T cells were illuminated with FRL for 6 hours per day for 2 days at different light intensities (0 to 2 mW/cm^2); scale bars, 50 μm. (**C**) Illumination time–dependent and (**D**) illumination intensity–dependent FICA-mediated genome editing of the endogenous gene *DNMT1*. The frequency of induced indel mutations was measured using a T7E1 assay 48 hours after the first illumination. The red arrowheads indicate the expected product cleaved by T7E1. One representative gel image of two individual experiments is shown. Data in (A) and (B) are expressed as means ± SD; $n = 3$ independent alignment. *P* values were calculated using a Student's *t* test. $^*P < 0.05$, $^{**}P < 0.01$, and $^{****}P < 0.0001$, FRL versus dark. Detailed descriptions of the genetic components and the transfection mixtures are provided in tables S1 and S5.

editing efficiency of Cas12a by stabilizing the formation of the ribonucleoprotein complexes (*51*). Therefore, we hypothesized that a U-rich sequence introduced between the MS2 loop and the crRNA would lead to increased transcriptional activation. Therefore, we designed two kinds of crRNAs with MS2 aptamers using U-rich sequences (crRNA–U-rich–MS2 or MS2–U-rich–crRNA) (fig. S7C). Our results showed that both of them were able to provide gene activation of the exogenous SEAP reporter and the up-regulation of the human endogenous *HBB*. Moreover, we found a further improvement when using two mixed crRNAs versus a single crRNA (fig. S7, D and E). Although this construct achieved a 44-fold increase in endogenous *HBB* compared with the dark group, there is apparently still room to improve the activation efficiency, as the design that recruiting multiple copies of the transcriptional activation domain has potential to increase gene expression (*52*).

To further improve the activation efficiency, we designed a photoactivatable dCas12a based on the SunTag system (Fig. 3A). Previous studies demonstrated that the SunTag system can be developed to enhance gene expression using an array of 10 amino acid copies of the starvation-responsive transcription factor GCN4 and recruiting multiple copies of scFv fused with a transcriptional activator. Hence, we further constructed three configurations of the FIdCA system using a constitutive promoter (P_{SV40})–driven dCas12a-GCN4 fusion protein and an FRL-activated scFv-activator fusion protein; or an FRL-activated dCas12a-GCN4 fusion protein and a P_{SV40}-driven scFv-activator fusion protein; or both an FRL-activated dCas12a-GCN4 fusion protein and an FRL-activated scFv-activator fusion protein. After this, we tested which combination showed stronger gene activation. Our results demonstrated that SEAP reporter expression could be efficiently activated under FRL using FRL-activated dCas12a-GCN4 fusion protein and a P_{SV40}-driven scFv-activator fusion protein (fig. S8).

To obtain an even more robust FIdCA system, we further optimized the aforementioned system using scFv fused with different transactivators, including p65-HSF1, VPR, VP64 (a tetrameric repeat of the minimal *Herpes simplex*–derived transactivator VP16), p65, and VP16 (herpes simplex viral protein 16). We found that scFv fused with p65-HSF1 resulted in the highest induction efficiency (12.0-fold) of SEAP expression upon FRL and relative low background in the dark (Fig. 3, B and C). In addition, we tested several FRL-responsive chimeric promoter variants with different copies of BldD-specific binding sequence and found that driving dCas12a-GCN4 fusion under the control of the P_{FRL3} [$(OwhiG)_2$-$P_{hCMVmin3G}$] promoter resulted in a highly efficient exogenous gene activation (Fig. 3D and fig. S9A). For further improvement, we fused the p65-HSF1 activators with nuclear localization signal (NLS) or nuclear export signal (NES) and found that scFv-p65-HSF1 without NLS and NES showed the highest FRL-triggered SEAP production (Fig. 3E and fig. S9B). Furthermore, we constructed a crRNA in multiplex single transcript that targeted the endogenous *HBB* gene. After optimizing the plasmid ratios of this modified system, we observed that FRL activated *HBB* by over 100-fold (Fig. 3F and fig. S10).

Characterization of the FIdCA system

We further assessed the performance of the FIdCA system. First, we assessed the kinetics of the FIdCA system and found that both the exogenous SEAP reporter gene expression (Fig. 4, A and C) and the activation of the endogenous *HBB* gene (Fig. 4, B and D) depended

Downloaded from https://www.science.org at Shanghai Normal University on December 16, 2021

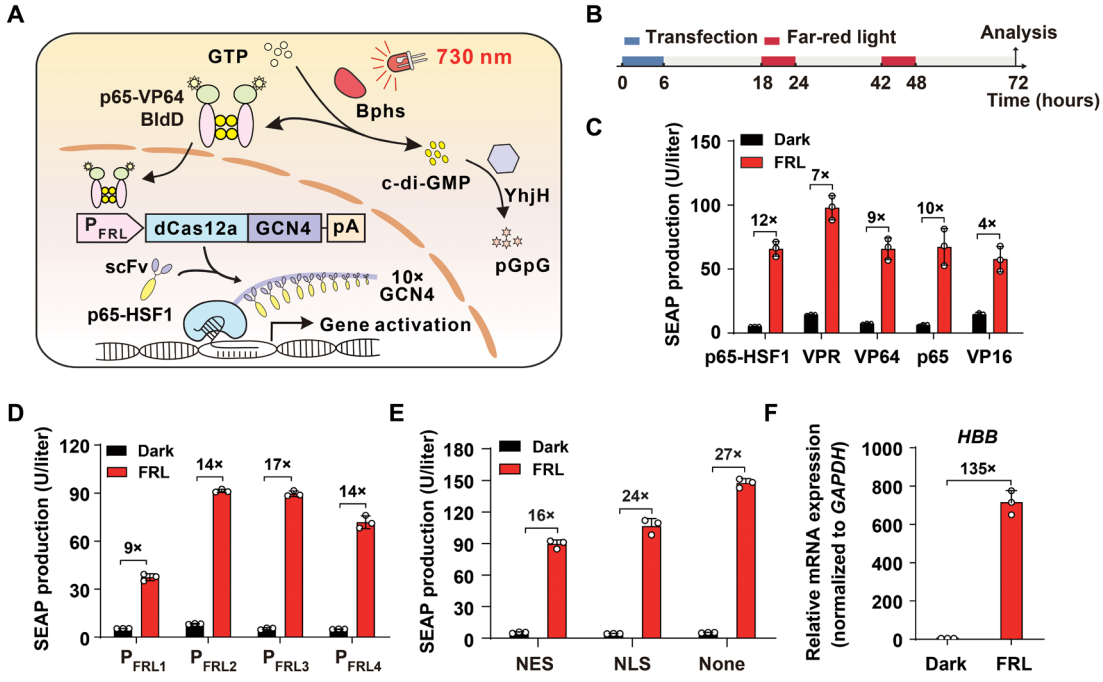


Fig. 3. Design and optimization of a FIdCA system. (**A**) Schematic design of the FIdCA system for gene activation. The FRL-specific chimeric promoter (P_{FRL}) initiated the expression of dCas12a fused with a 10× repeating GCN4 peptide. An scFv antibody fused with the transcriptional activation domain (p65-HSF1) driven by the P_{hCMV} can be recruited to the tandem repeat region of the GCN4 peptide fused with dCas12a to initiate transcriptional activation under FRL. (**B**) Time schedule for the experimental procedure of FIdCA-mediated gene activation. (**C**) Screening different transcriptional activators fused with scFv for gene activation. SEAP production was quantified 48 hours after the first illumination. (**D**) Optimization of different FRL-responsive P_{FRLX}-driven dCas12a-GCN4 expression. SEAP production was quantified 48 hours after the first illumination. (**E**) Optimization of the nuclear signals of scFv-p65-HSF1. SEAP production was quantified 48 hours after the first illumination. (**F**) Activation of the endogenous *HBB* gene by the optimized FIdCA system. The relative mRNA expression of *HBB* was quantified by quantitative polymerase chain reaction (PCR) 48 hours after the first illumination. Data in (C) to (F) are expressed as means ± SD; $n = 3$ independent experimental replicates. Detailed descriptions of the genetic components and the transfection mixtures are provided in tables S1 and S5.

on the intensity and time of exposure to FRL. Furthermore, the FIdCA system enabled reversible control of the expression of exogenous and endogenous genes (Fig. 4, E and F) and showed a spatial transgene activation upon local illumination (Fig. 4G). After this, we transfected the FIdCA system into different cell lines and found that it was functional in a number of mammalian cell types (fig. S11), which demonstrates the wide applicability and compatibility of the FIdCA system.

Specifically, to evaluate the photocytotoxicity of FRL (730 nm) or blue light (460 nm) illumination on the viability of mammalian cells, we transfected HEK-293T cells with a constitutive SEAP expression vector (pSEAP2-control) and then illuminated these cells with either FRL (2 mW/cm^2) or blue light at different light intensities (0 to 2 mW/cm^2) for 6 hours. SEAP production revealed that FRL resulted in neglectable cytotoxicity at higher light intensity (2 mW/cm^2), while blue light markedly decreased the amount of SEAP expression at light intensities above 0.25 mW/cm^2. In addition, we did not observe a substantial increase in cytotoxicity after extended FRL exposure of cells equipped with either the FICA or the FIdCA system. However, we did observe a decrease in cell viability following blue light irradiation at a light intensity above 0.25 mW/cm^2, indicating that FRL is considerably less phototoxic to mammalian cells when compared with blue light (fig. S12). Moreover, our results showed that the FIdCA system induced significant SEAP expression under FRL (730 nm) illumination, which underlines the chromatic specificity of the FIdCA system (fig. S13).

Last, we have further compared the activation efficiency between the FIdCA and FACE systems in HEK-293T cells. The data revealed that the activation of the endogenous *HBB* gene using the FIdCA system was superior to that using the FACE system [*HBB*: 112-fold (FIdCA) versus 11-fold (FACE)] (fig. S14). These results imply that the FIdCA system has the potential to activate some endogenous genes more efficiently than FACE system.

FIdCA-mediated gene activation in vivo

We subsequently tested whether the FIdCA system was able to activate transgene expression in vivo upon FRL. To facilitate in vivo FIdCA system delivery, we generated an iteration of the single plasmid that concatenated the constructs for crRNA and dCas12a-GCN4 or scFv-p65-HSF1 and luciferase reporter. After this, we cotransfected HEK-293T cells with three plasmids: the FRL-responsive sensor pXY137, the concatenated dCas12a vector pZQ303, and the concatenated transactivator and reporter vector pZQ304. We found that this combination showed higher background luciferase expression in dark conditions (fig. S15). To reduce the background activity, we constructed a luciferase reporter driven by the weaker P_{TATA} promoter pZQ315 and found that HEK-293T cells cotransfected with the luciferase reporter under the control of the P_{TATA} promoter exhibited lower background activity in dark conditions (fig. S16).

We then transiently transfected C57BL/6 mice with the FIdCA system comprising the FRL-responsive sensor pXY137, the concatenated

Downloaded from https://www.science.org at Shanghai Normal University on December 16, 2021

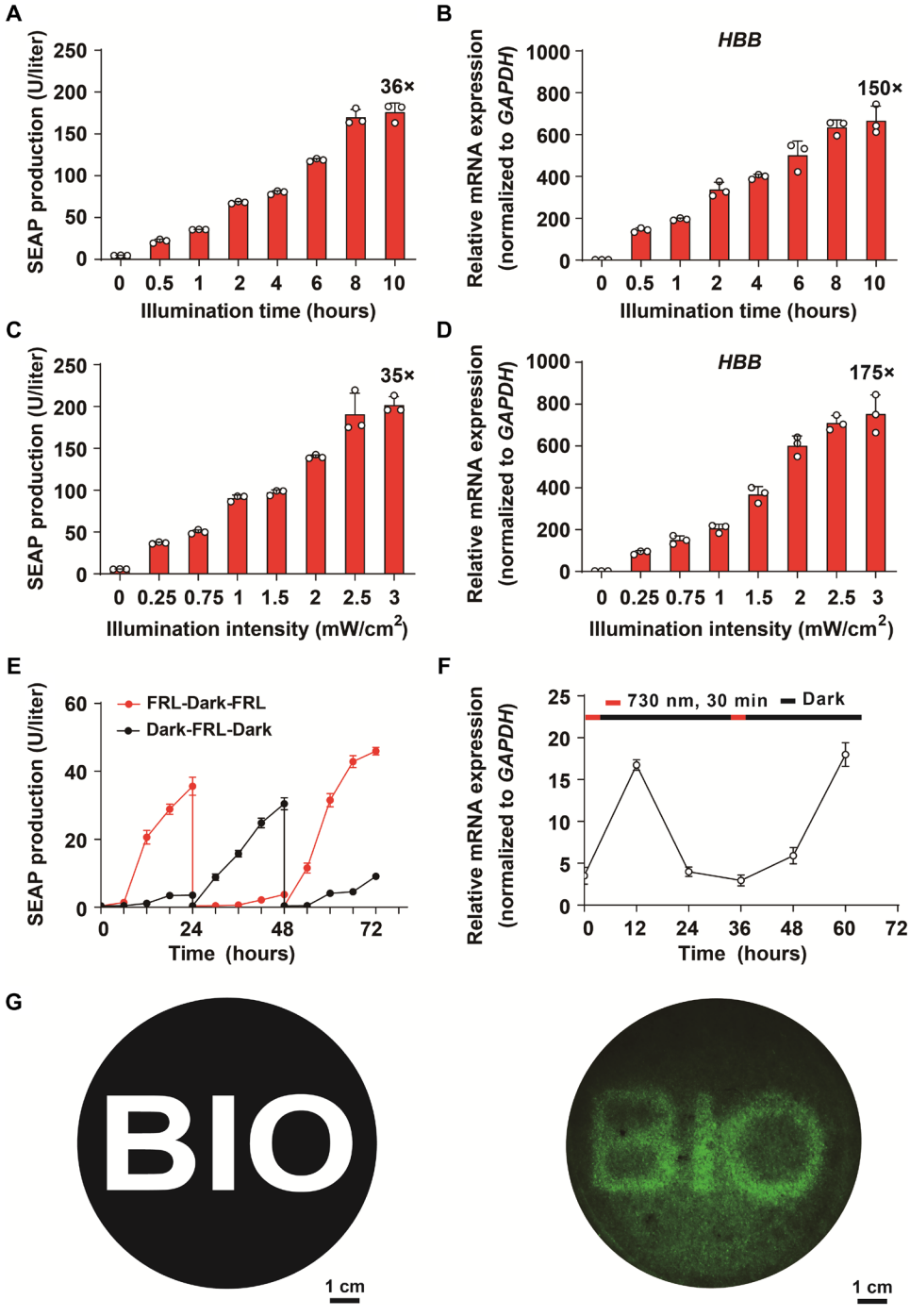


Fig. 4. Characterization of the FIdCA system. (**A** and **B**) Exposure time-dependent FIdCA-mediated activation of the exogenous (A) and endogenous (B) gene expression. Transfected HEK-293T cells were illuminated with FRL (730 nm, 2 mW/cm^2) for different time periods (0 to 10 hours per day) for 2 days. (**C** and **D**) Illumination intensity–dependent FIdCA-mediated activation of the exogenous (C) and endogenous (D) gene expression. Transfected HEK-293T cells were illuminated with FRL for 6 hours per day for 2 days at different light intensities (0 to 3 mW/cm^2). (**E** and **F**) Reversibility of FIdCA-mediated transgene expression. Transfected HEK-293T cells were illuminated with FRL (730 nm, 2 mW/cm^2) for 30 min (on) or instead kept in the dark (off). The exogenous SEAP expression was quantified every 6 hours for 72 hours, and the culture medium was changed every 24 hours. The endogenous *HBB* mRNA expression was quantified by qPCR every 12 hours for 60 hours. (**G**) Spatial control of FRL-dependent transgene expression mediated by the FIdCA system; scale bars, 1 cm. Data in (A) to (F) are expressed as means ± SD; $n = 3$ independent experimental replicates. Detailed descriptions of the genetic components and the transfection mixtures are provided in tables S1 and S5.

Downloaded from https://www.science.org at Shanghai Normal University on December 16, 2021

dCas12a vector pZQ303, and the integrated transactivator and reporter pZQ315 (Fig. 5A), using hydrodynamic injection via the tail vein. Eight hours after the injection, the abdomens of the transfected mice were either illuminated with FRL for 8 hours (730 nm, 10 mW/cm^2, 2 min on, 2 min off, alternating) or kept in the dark and (Fig. 5B). We found that the mice exposed to FRL exhibited higher luciferase activity in the livers compared with those kept in the dark. Furthermore, quantitative analysis of bioluminescence imaging revealed that the mice injected under FRL exhibited notably increased luciferase activity (Fig. 5, C and D). These results demonstrated that our FIdCA system is able to activate target genes in vivo using noninvasive LED.

DISCUSSION

CRISPR-Cas9 emerged as a powerful technology that has been widely used for the modification of the mammalian genome. Cas12a is also an RNA-guided DNA nuclease but has distinctive characteristics from Cas9. Specifically, Cas12a can autonomously process crRNA arrays from a single transcript, recognize a T-rich PAM, and then generate sticky ends. These unique features make CRISPR-Cas12a a promising gene editing tool and a potential alternative to CRISPR-Cas9. However, in contrast to Cas9, the difficulties in developing an efficient and modified Cas12a limit its current applications. We explored the potential applicability of Cas12a by developing FICA/FIdCA systems with negligible phototoxicity, deep tissue penetrative capability, and good biocompatibility for tunable genome editing in mammalian cells and for transcriptional activation in both mammalian cells and mice.

Moreover, the use of LED lights satisfies the criteria for safe medical applications in humans and does not necessitate invasive techniques, such as injury to the skull or skin, for implanting optic fiber. Hence, the advantages of our systems can facilitate in vivo experiments and reduce common side effects resulting from cytotoxicity or physical lesions in the organisms.

In addition to genome editing, the dCas12a-mediated gene activation was achieved by fusing different transactivators to dCas12a to promote genome regulation. A previous study developed a potent dCas9 activator and demonstrated that transcriptional activators

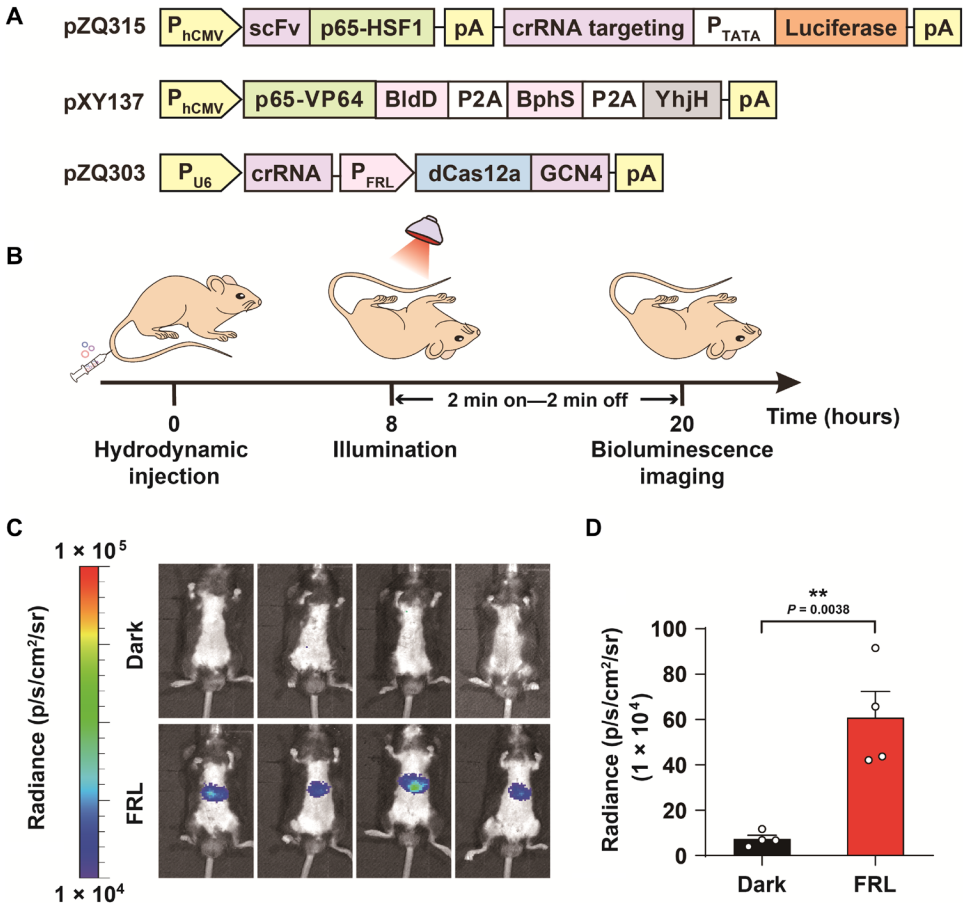


Fig. 5. FIdCA-mediated gene activation in mice. (**A**) Schematic representation of the genetic configuration for the FIdCA system used in mice. (**B**) Schematic representation of the experimental procedure and the time schedule used for evaluating in vivo gene activation. Plasmids (pZQ315, pXY137, and pZQ303) expressing the iteration of the FIdCA system were transiently transfected into mice by hydrodynamic tail vein injection. Eight hours after injection, the mice were illuminated with FRL (10 mW/cm^2, 730 nm, 2 min on, 2 min off) or instead maintained in the dark. Bioluminescence imaging was performed 20 hours after hydrodynamic injection. (**C**) Bioluminescence IVIS image of the luciferase reporter gene activation in mice transfected with the FIdCA system. (**D**) Quantification of the bioluminescence activity shown in (C). Data in (D) are expressed as means ± SEM; $n = 4$ mice. P values were calculated using a Student's t test. $^{**}P < 0.01$, FRL versus dark. Detailed descriptions of the genetic components and the transfection mixtures are provided in tables S1 and S5.

Downloaded from https://www.science.org at Shanghai Normal University on December 16, 2021

improve the activation efficiency of dCas9 activators. Accordingly, we have developed the FIdCA system by fusing dCas12a with three different activators to activate gene expression: VPR, SAM, and SunTag. Our results show that the FIdCA system based on VPR and SAM had relatively low gene activation upon FRL (figs. S6 and S7). A possible reason for this observation is that these constructions are only able to recruit one copy of the transactivator, which may be insufficient for induction of endogenous gene expression upon FRL.

Subsequently, we designed a photoactivatable dCas12a based on the SunTag system that could enhance gene expression using an array of 10 amino acid copies of the starvation-responsive transcription factor GCN4 and recruit multiple copies of the scFv antibody fused with transcriptional activators (*52*). We successfully established a FIdCA system that comprises a FIdCA-GCN4 and constitutively expressed scFv-activators. Our FIdCA system can effectively activate the expression of endogenous genes upon FRL and has spatial and temporal control capacities.

Red/FRL-responsive optogenetic devices reported to date have been based on PhyB/PIF6 derived from *Arabidopsis thaliana* (*53*, *54*) and BphP1/PpsR2 (or an engineered QPAS1) derived from *Rhodopseudomonas palustris* (*55*, *56*); there is also a recently reported near-infrared optogenetic system based on IsPadC-PCM from *Idiomarina* sp. *A28L* (*57*). Recall that our FICA/FIdCA system is based on the bacterial photoreceptor BphS and the CRISPR system Cas12a. A distinction bears emphasis here: The previously reported systems have been applied for gene transcription activation based on the GAL4-UAS system or the Tet repressor–based system. However, none of these red/FRL systems have been applied for CRISPR-Cas12a–mediated gene editing and gene activation. We have for some time been investigating FRL-inducible genetic systems, and we here report our development of the FIdCA system, which achieved noninvasive gene activation in mice based on Cas12a.

There is still room for improvement with regard to the efficiency and convenience of our FICA/FIdCA system. Advancement of in vivo delivery strategies, including, for example, selecting capsid variants of adeno-associated viruses (AAVs) (*58*) or using nonviral vectors including engineered extracellular vehicles (*59*), may help increase the efficiency of delivery for our system to targeted tissues. It is also possible that a more packable optogenetic device such as the single-component near-infrared optogenetic system (*57*) might provide a new direction for improving CRISPR-based gene activation levels in vivo. Note that recently reported small-size Cas proteins [Cas 13bt (*60*), Cas12f1 (*61*), etc.] should work well with our system for in vivo applications. We anticipate that our system will expand the application scope for CRISPR-Cas12a–based technologies from fundamental studies toward biomedical translational research.

MATERIALS AND METHODS

Construction of the FICA system

The constructs were assembled by standard molecular cloning techniques. Cas12a derived from *Acidaminococcus* sp. *BV3L6* was amplified from the Addgene plasmid 69982 and cloned downstream of the FRL-responsive promoter P_{FRL} using Eco RI and Hind III sites.

Construction of the FIdCA system

To generate the FIdCA system, the E993A mutation was introduced in Cas12a by overlap polymerase chain reaction (PCR). The 10 amino acid copies of the starvation-responsive transcription factor GCN4 fragment were amplified from the Addgene plasmid 78899 and ligated to the C terminus of dCas12a with a glycine-serine linker and an NLS. The scFv and p65-HSF1 fragments were amplified by standard PCR and then fused to the glycine-serine linker sequences using the MultiS One Step Cloning Kit (Vazym, Nanjing, China, catalog no. C113-01) according to the manufacturer's instructions. All genetic components were confirmed by sequencing (Genewiz Inc., Suzhou, China). Detailed information on the plasmids constructed in this study is provided in table S1.

Construction of crRNAs and sgRNAs

The crRNAs targeting *DNMT1*, *FANCF*, *GRIN2B*, *CXCR*, *HBB*, *d2EYFP*, *SEAP*, and *EGFP* were generated by the annealed oligo cloning strategy using the Bsm BI site of a constitutive P_{U6}-driven crRNA vector (pZQ23) (*19*, *21*). The P_{U6}-crRNA cassette was amplified from the Addgene plasmid 78741 and cloned into pcDNA3.1 (+). For the construction of crRNAs bearing MS2 RNA aptamers, we generated crRNAs targeting *HBB* and *SEAP* with MS2 aptamers (Addgene no. 102560) by the annealed oligo cloning strategy using the Bsm BI site of the pZQ23 vector. The sgRNAs targeting *IL12A-AS1* and *PRKCH* were constructed as previously described (*37*). The sgRNAs targeting *HBB* were constructed as previously described (*36*). For the construction of crRNA array, we designed oligonucleotides for one-directional annealing through their sticky ends. The oligonucleotides (final concentration, 10 μM) were mixed with 10× Primer start buffer (Takara, Dalian, China, catalog no. R010A) to 20 μl. The mixture was phosphorylated and annealed on a thermocycler (95°C, 5 min; 94°C, 2 s, −0.1°C per cycle, 200 times; 75°C, 1 s, −0.1°C per cycle, 600 times; 16°C, 5 min). The annealed pre-crRNA array was ligated to a pZQ23 using the Bsm BI site. The target sequences that were used for constructing the crRNA are provided in table S2.

Cell culture and transfection

HEK cells (HEK-293T; American Type Culture Collection, CRL-11268) were cultured in Dulbecco's modified Eagle's medium (Gibco, NY, USA, catalog no. 31600-083), supplemented with 10% (v/v) fetal bovine serum (Gibco, catalog no. 10270-106) and a 1% (v/v) penicillin and streptomycin solution (Beyotime Inc., Shanghai, China, catalog no. ST488-1/ST488-2). Cells were cultured at 37°C in a humidified atmosphere containing 5% CO_2. The cells were regularly tested for the absence of *Mycoplasma* and bacterial contamination. Transfections were performed using an optimized polyethyleneimine (PEI)–based protocol. Briefly, a total of 6×10^4 cells per well were seeded into a 24-well cell culture plate without exogenous supplement of biliverdin for 18 hours before transfection and then cotransfected with the corresponding plasmid mixtures for 6 hours with 50 μl of 3:1 PEI:DNA mixture (PEI; molecular weight, 40,000; stock solution, 1 mg/ml in ddH_2O; catalog no. 24765, Polysciences). The concentration and viability of the cell lines were evaluated with a Countess II Automated cell counter (Life Technologies, USA).

SEAP reporter assay

The production of human placental SEAP in the cell culture was quantified using a p-nitrophenylphosphate–based light absorbance time course assay. Briefly, the cell supernatants were collected and heated for 30 min at 65°C to inactivate the cell culture supernatant. We added 120 μl of substrate solution [100 μl of 2× SEAP buffer containing 20 mM homoarginine, 1 mM $MgCl_2$, and 21% (v/v) diethanolamine (pH 9.8), and 20 μl of p-nitrophenylphosphate substrate solution containing

Downloaded from https://www.science.org at Shanghai Normal University on December 16, 2021

120 mM p-nitrophenylphosphate] to 80 μl of the heat-inactivated supernatants. The absorbance was measured at 405 nm using a Synergy H1 hybrid multimode microplate reader (BioTek Instruments Inc., USA) installed with the Gen5 software (version 2.04).

FICA-mediated gene editing activity in HEK-293T

For FRL-controlled exogenous gene editing experiments, HEK-293T cells (6×10^4) were cotransfected with pXY137 (P_{hCMV}-p65-VP64-BldD-pA-P_{hCMV}-BphS-P2A-YhjH-pA), pDL192 (P_{FRL2}-h_{CMVmin}-Cas12a-pA), and pDL196 (P_{SV40}-d2EYFP-pA), together with pDL194 (P_{U6}-crRNA1$_{d2EYFP}$-pA) and pDL197 (P_{U6}-crRNA2$_{d2EYFP}$-pA). The cells were then illuminated with FRL (730 nm, 2 mW/cm^2) for 6 hours per day for 2 days. The expression of the d2EYFP reporter was visualized by fluorescence microscopy and quantified by flow cytometry 48 hours after the first illumination.

For FRL-controlled endogenous gene editing experiments, HEK-293T cells (6×10^4) were cotransfected with pXY137, pDL192, and pZQ28 (P_{U6}-crRNA$_{DNMT1}$-pA), pZQ206 (P_{U6}-crRNA$_{FANCF}$-pA), pZQ205 (P_{U6}-crRNA$_{GRIN2B}$-pA), or pZQ288 (P_{U6}-crRNA$_{CXCR}$-pA) and illuminated with FRL (730 nm, 2 mW/cm^2) for 6 hours per day for 2 days. The frequency of induced indel mutations was measured by a T7E1 assay 48 hours after the first illumination.

Mismatch-sensitive T7E1 assay

Genomic DNA was extracted from the cells using the TIANamp Genomic DNA Extraction Kit (TIANGEN Biotech Inc., Beijing, China, catalog no. DP304) according to the manufacturer's instructions. The genomic region containing the target sequence was amplified by PCR with a 2× Taq Plus Master Mix II (Dye Plus) DNA polymerase (Vazyme, catalog no. P213). The PCR primers that were used for each target gene are shown in table S3. The amplified PCR products were purified using HiPure Gel Pure Micro Kits (Magen Inc., Shanghai, China, catalog no. D2111-03). To promote restriction enzyme, we mixed 500 ng of purified DNA products with 1.5 μl of 10× M Buffer (Takara, catalog no.1093A) and Milli-Q water to a final volume of 15 μl. The DNA was then reannealed to form heteroduplex DNA (95°C, 5 min; 94°C, 2 s, –0.1°C per cycle, 200 times; 75°C, 1 s, –0.1°C per cycle, 600 times; 16°C, 5 min), which was subjected to 5 U of T7E1 endonuclease I digestion (New England Biolabs, catalog no. M0302) for 30 min at 37°C, and, lastly, analyzed by 1.5% agarose gel electrophoresis. The gels were stained with GelRed (Vazyme, catalog no. GR501-01) and visualized using a Tanon 3500 gel imaging system (Tanon Science & Technology Inc.). The proportion of indel mutation promoted by Cas12a was calculated using the ImageJ software with the following formula: $100\% \times [1 - (1 - (b + c)/(a + b + c))^{1/2}]$, in which a is the integrated intensity of the undigested PCR product, and b and c are the integrated intensities of the T7E1-digested products.

TIDE analysis

Target regions were amplified from genomic DNA by PCR using 2× Taq Plus Master Mix II (Dye Plus) DNA polymerase (Vazyme, catalog no. P213). Purified PCR products were analyzed by Sanger sequencing. The ab1 Sanger sequencing files were uploaded to the online TIDE analysis tool (https://tide.nki.nl/) (*62*) to quantify the nature and frequency of the generated indels.

Targeted deep sequencing

Targeted regions were amplified from genomic DNA using 2× Taq Plus Master Mix II (Dye Plus) DNA polymerase (Vazyme, catalog no. P213). The paired-end sequencing of PCR amplicons was performed on Illumina MiSeq (Sangon Biotech, Shanghai). The PCR primers used for the amplification of regions for deep sequencing are provided in table S4. The average depth of coverage for the sequencing runs was ~20,000 reads. The paired-end MiSeq raw data were analyzed using the SSH Secure Shell Client software from Sangon Biotech.

Quantitative real-time PCR analysis

Total RNA was isolated using the RNAiso Plus Kit (Takara, catalog no.9109) according to the manufacturer's instructions. A total of 500 ng of mRNA was reverse transcribed into cDNA using the PrimeScript RT Reagent Kit with the genomic DNA Eraser (Takara, catalog no. RR047). Quantitative PCR (qPCR) analysis was performed on a real-time PCR instrument (Roche, LightCycler 96, Switzerland) using the SYBR Premix Ex Taq (Takara, catalog no. RR420) to detect each of the target genes. The list of qPCR primers used in this study is available in table S4. We used the following PCR cycling parameters: 95°C for 5 min, followed by 40 cycles of 95°C for 10 s, 60°C for 30 s. Samples that were transfected with AsCas12a crRNA backbone plasmid (pZQ23) were used as negative controls. The relative cycle threshold (CT) of the housekeeping gene human *glyceraldehyde 3-phosphate dehydrogenase* (*GAPDH*) was measured as an endogenous control, and thus, the relative mRNA expression levels were normalized to match those of *GAPDH* using the standard $\Delta\Delta C_t$ method.

Flow cytometry analysis

The transfected HEK-293T cells were dissociated by 0.25% Trypsin-EDTA (Sangon Biotech, Shanghai, China, catalog no. AP10629-0050) for 3 min and then washed in phosphate-buffered saline for three consecutive times. The resuspended cells were analyzed using a Becton Dickinson LSRFortessa Flow Cytometer (BD Biosciences, San Jose, USA) equipped for EGFP/d2EYFP [488-nm laser, 505-nm long pass filter, and 530/30 emission filter (passband centered on 530 nm; passband width, 30 nm)]. Approximately 10,000 cells per sample were recorded, and the data were analyzed by the FlowJo software (version no. 7.6). The transfected HEK-293T cell populations were gated for cells with high EGFP/d2EYFP fluorescence beyond a threshold of 10^3 arbitrary fluorescence units. The expression values of weighted EGFP/d2EYFP were calculated as the percentage of gated cells multiplied by their median fluorescence, which is correlated with fluorescence intensity and cell number.

Fluorescence microscopy

Fluorescence microscopy images of the cells expressing d2EYFP/EGFP were obtained using an inverted fluorescence microscope (Leica DMI8, Wetzlar, Germany) with a 20× objective and a 495/535-nm (B/G/R) excitation/emission filter set. Identical settings, including exposure times for d2EYFP/EGFP, were used for all fluorescence micrographs.

FIdCA-mediated gene activation in mammalian cells

For FRL-controlled exogenous SEAP reporter experiments, HEK-293T cells (6×10^4) were cotransfected with the pXY137, pZQ113 (P_{hCMV}-scFv-p65-HSF1-pA), pZQ116 (P_{FRL3}-dCas12a-NLS-GCN4-pA), pZQ28 (P_{U6}-crRNA$_{SEAP}$-pA), and pZQ5 (crRNA targeting site-$P_{hCMVmin}$-SEAP-pA). The cells were subsequently illuminated with FRL (730 nm, 2 mW/cm^2) for 6 hours per day for 2 days. SEAP production levels in the culture medium were quantified 48 hours after the first illumination.

Downloaded from https://www.science.org at Shanghai Normal University on December 16, 2021

For FRL-controlled endogenous gene experiments, HEK-293T cells (6×10^4) cotransfected with the pXY137, pZQ113, pZQ116, and pZQ34 (P_{U6}-crRNA$_{HBB}$-pA) were illuminated with FRL (730 nm, 2 mW/cm^2) for 6 hours per day for 2 days, and the relative mRNA expression of *HBB* was quantified by qPCR 48 hours after the first illumination.

Spatial control of FRL-dependent gene activation in mammalian cells

HEK-293T cells (3×10^6) were plated into a 10-cm dish, cultivated overnight to 60 to 70% confluency, and then transfected with 1000 μl of a 3:1 PEI:DNA mixture (w/w) containing 15 μg of plasmid DNA [pXY137, pDL247, pZQ5, pZQ113, and pZQ116 at a ratio of 5:3:3:2:3 (w/w/w/w/w)]. Twenty-four hours after transfection, the cells were illuminated with FRL for 24 hours (730 nm, 0.5 mW/cm^2, 1 min on, 5 min off) under a "BIO"-patterned photomask made from aluminum foil. The patterned photomask was placed between the upward-facing LED array and the bottom of the 10-cm culture dish. Fluorescence images were obtained 24 hours after illumination using the ChemiScope 4300 Pro imaging equipment (Clinx, Shanghai, China).

In vivo gene activation using FIdCA system

We randomly divided male wild-type C57BL/6 mice [6 weeks old; East China Normal University (ECNU) Laboratory Animal Center] into two groups. Before injecting the mice, the plasmids encoding the FIdCA system [pXY137, pZQ303, and pZQ315 at a 2:4:1(w/w/w) ratio] were mixed into a Ringer's solution (147 mM NaCl, 4 mM KCl, and 1.13 mM $CaCl_2$) Each mouse was hydrodynamically injected with 350 μg of DNA without exogenous supplement of biliverdin within 8 s via tail vein. The injection volume of the plasmid solution was 2 ml per mouse weight (20 ± 2 g). Eight hours after injection, the mice were exposed to FRL (730 nm LED, 10 mW/cm^2, 2 min on, 2 min off, alternating). Control mice were kept in the dark. Twelve hours after illumination, each mouse was intraperitoneally injected with 100 μl of Hanks' balanced salt solution supplemented with 100 mM luciferin substrate solution (Synchem, CAS no. 115144-35-9) and anesthetized with ether before proceeding with imaging. Ten minutes after luciferin injection, we obtained bioluminescence images of the mice using the IVIS Lumina II in vivo imaging system (PerkinElmer, USA).

Ethics

The animal experiments were approved by the ECNU Animal Care and Use Committee and in direct accordance with the Ministry of Science and Technology of the People's Republic of China on Animal Care guidelines. The protocol (protocol ID: m20191212) was approved by the ECNU Animal Care and Use Committee. All mice were euthanized after the completion of the experiments.

Statistical analysis

All in vitro data represent the means ± SD and are described separately in the figure legends. For the animal experiments, the results are expressed as the means ± SEM. Comparisons between the groups were performed using a Student's *t* test. Differences were considered statistically significant at $P < 0.05$ (*), very significant at $P < 0.01$ (**), and extremely significant at $P < 0.001$ (***). The Prism 5 software (version 6, GraphPad Software) was used for statistical analysis. *n* and *P* values are provided in the figure legends.

SUPPLEMENTARY MATERIALS

Supplementary material for this article is available at https://science.org/doi/10.1126/sciadv.abh2358

View/request a protocol for this paper from *Bio-protocol*.

REFERENCES AND NOTES

1. M. Jinek, K. Chylinski, I. Fonfara, M. Hauer, J. A. Doudna, E. Charpentier, A programmable dual-RNA-guided DNA endonuclease in adaptive bacterial immunity. *Science* **337**, 816–821 (2012).
2. L. S. Qi, M. H. Larson, L. A. Gilbert, J. A. Doudna, J. S. Weissman, A. P. Arkin, W. A. Lim, Repurposing CRISPR as an RNA-guided platform for sequence-specific control of gene expression. *Cell* **152**, 1173–1183 (2013).
3. L. Cong, F. A. Ran, D. Cox, S. Lin, R. Barretto, N. Habib, P. D. Hsu, X. Wu, W. Jiang, L. A. Marraffini, F. Zhang, Multiplex genome engineering using CRISPR/Cas systems. *Science* **339**, 819–823 (2013).
4. P. D. Hsu, E. S. Lander, F. Zhang, Development and applications of CRISPR-Cas9 for genome engineering. *Cell* **157**, 1262–1278 (2014).
5. M. Tabebordbar, K. Zhu, J. K. W. Cheng, W. L. Chew, J. J. Widrick, W. X. Yan, C. Maesner, E. Y. Wu, R. Xiao, F. A. Ran, L. Cong, F. Zhang, L. H. Vandenberghe, G. M. Church, A. J. Wagers, In vivo gene editing in dystrophic mouse muscle and muscle stem cells. *Science* **351**, 407–411 (2016).
6. H. Ma, N. Marti-Gutierrez, S.-W. Park, J. Wu, Y. Lee, K. Suzuki, A. Koski, D. Ji, T. Hayama, R. Ahmed, H. Darby, C. Van Dyken, Y. Li, E. Kang, A. R. Park, D. Kim, S.-T. Kim, J. Gong, Y. Gu, X. Xu, D. Battaglia, S. A. Krieg, D. M. Lee, D. H. Wu, D. P. Wolf, S. B. Heitner, J. C. I. Belmonte, P. A. Mato, J.-S. Kim, S. Kaul, S. Mitalipov, Correction of a pathogenic gene mutation in human embryos. *Nature* **548**, 413–419 (2017).
7. X. Gao, Y. Tao, V. Lamas, M. Huang, W.-H. Yeh, B. Pan, Y.-J. Hu, J. H. Hu, D. B. Thompson, Y. Shu, Y. Li, H. Wang, S. Yang, Q. Xu, D. B. Polley, M. C. Liberman, W.-J. Kong, J. R. Holt, Z.-Y. Chen, D. R. Liu, Treatment of autosomal dominant hearing loss by in vivo delivery of genome editing agents. *Nature* **553**, 217–221 (2018).
8. C. E. Nelson, Y. Wu, M. P. Gemberling, M. L. Oliver, M. A. Waller, J. D. Bohning, J. N. Robinson-Hamm, K. Bulaklak, R. M. C. Rivera, J. H. Collier, A. Asokan, C. A. Gersbach, Long-term evaluation of AAV-CRISPR genome editing for Duchenne muscular dystrophy. *Nat. Med.* **25**, 427–432 (2019).
9. B. Zetsche, J. S. Gootenberg, O. O. Abudayyeh, I. M. Slaymaker, K. S. Makarova, P. Essletzbichler, S. E. Volz, J. Joung, J. van der Oost, A. Regev, E. V. Koonin, F. Zhang, Cpf1 is a single RNA-guided endonuclease of a class 2 CRISPR-Cas system. *Cell* **163**, 759–771 (2015).
10. T. Yamano, H. Nishimasu, B. Zetsche, H. Hirano, I. M. Slaymaker, Y. Li, I. Fedorova, T. Nakane, K. S. Makarova, E. V. Koonin, R. Ishitani, F. Zhang, O. Nureki, Crystal structure of Cpf1 in complex with guide RNA and target DNA. *Cell* **165**, 949–962 (2016).
11. H. Jia, V. Orbovic, N. Wang, CRISPR-LbCas12a-mediated modification of citrus. *Plant Biotechnol. J.* **17**, 1928–1937 (2019).
12. X. Tang, Q. Ren, L. Yang, Y. Bao, Z. Zhong, Y. He, S. Liu, C. Qi, B. Liu, Y. Wang, S. Sretenovic, Y. Zhang, X. Zheng, T. Zhang, Y. Qi, Y. Zhang, Single transcript unit CRISPR 2.0 systems for robust Cas9 and Cas12a mediated plant genome editing. *Plant Biotechnol. J.* **17**, 1431–1445 (2019).
13. L. Dong, X. Guan, N. Li, F. Zhang, Y. Zhu, K. Ren, L. Yu, F. Zhou, Z. Han, N. Gao, Z. Huang, An anti-CRISPR protein disables type V Cas12a by acetylation. *Nat. Struct. Mol. Biol.* **26**, 308–314 (2019).
14. W. X. Yan, P. Hunnewell, L. E. Alfonse, J. M. Carte, E. Keston-Smith, S. Sothiselvam, A. J. Garrity, S. Chong, K. S. Makarova, E. V. Koonin, D. R. Cheng, D. A. Scott, Functionally diverse type V CRISPR-Cas systems. *Science* **363**, 88–91 (2019).
15. P. Gao, H. Yang, K. R. Rajashankar, Z. Huang, D. J. Patel, Type V CRISPR-Cas Cpf1 endonuclease employs a unique mechanism for crRNA-mediated target DNA recognition. *Cell Res.* **26**, 901–913 (2016).
16. B. Zetsche, M. Heidenreich, P. Mohanraju, I. Fedorova, J. Kneppers, E. M. DeGennaro, N. Winblad, S. R. Choudhury, O. O. Abudayyeh, J. S. Gootenberg, W. Y. Wu, D. A. Scott, K. Severinov, J. van der Oost, F. Zhang, Multiplex gene editing by CRISPR-Cpf1 using a single crRNA array. *Nat. Biotechnol.* **35**, 31–34 (2017).
17. Y. Jiang, F. Qian, J. Yang, Y. Liu, F. Dong, C. Xu, B. Sun, B. Chen, X. Xu, Y. Li, R. Wang, S. Yang, CRISPR-Cpf1 assisted genome editing of corynebacterium glutamicum. *Nat. Commun.* **8**, 15179 (2017).
18. M. Wang, Y. Mao, Y. Lu, X. Tao, J. K. Zhu, Multiplex gene editing in rice using the CRISPR-Cpf1 system. *Mol. Plant* **10**, 1011–1013 (2017).
19. D. Kim, J. Kim, J. K. Hur, K. W. Been, S. H. Yoon, J. S. Kim, Genome-wide analysis reveals specificities of Cpf1 endonucleases in human cells. *Nat. Biotechnol.* **34**, 863–868 (2016).
20. Y. Zhang, C. Long, H. Li, J. R. McAnally, K. K. Baskin, J. M. Shelton, R. Bassel-Duby, E. N. Olson, CRISPR-Cpf1 correction of muscular dystrophy mutations in human cardiomyocytes and mice. *Sci. Adv.* **3**, e1602814 (2017).
21. B. P. Kleinstiver, S. Q. Tsai, M. S. Prew, N. T. Nguyen, M. M. Welch, J. M. Lopez, Z. R. McCaw, M. J. Aryee, J. K. Joung, Genome-wide specificities of CRISPR-Cas Cpf1 nucleases in human cells. *Nat. Biotechnol.* **34**, 869–874 (2016).

Downloaded from https://www.science.org at Shanghai Normal University on December 16, 2021

22. D. Singh, J. Mallon, A. Poddar, Y. Wang, R. Tippana, O. Yang, S. Bailey, T. Ha, Real-time observation of DNA target interrogation and product release by the RNA-guided endonuclease CRISPR Cpf1 (Cas12a). *Proc. Natl. Acad. Sci. U.S.A.* **115**, 5444–5449 (2018).
23. Y. E. Tak, B. P. Kleinstiver, J. K. Nunez, J. Y. Hsu, J. E. Horng, J. Gong, J. S. Weissman, J. K. Joung, Inducible and multiplex gene regulation using CRISPR-Cpf1-based transcription factors. *Nat. Methods* **14**, 1163–1166 (2017).
24. J. S. Chen, E. Ma, L. B. Harrington, M. Da Costa, X. Tian, J. M. Palefsky, J. A. Doudna, CRISPR-Cas12a target binding unleashes indiscriminate single-stranded DNase activity. *Science* **360**, 436–439 (2018).
25. P. C. DeWeirdt, K. R. Sanson, A. K. Sangree, M. Hegde, R. E. Hanna, M. N. Feeley, A. L. Griffith, T. Teng, S. M. Borys, C. Strand, J. K. Joung, B. P. Kleinstiver, X. Pan, A. Huang, J. G. Doench, Optimization of AsCas12a for combinatorial genetic screens in human cells. *Nat. Biotechnol.* **39**, 94–104 (2021).
26. K. Lee, Y. Zhang, B. P. Kleinstiver, J. A. Guo, M. J. Aryee, J. Miller, A. Malzahn, S. Zarecor, C. J. Lawrence-Dill, J. K. Joung, Y. Qi, K. Wang, Activities and specificities of CRISPR/Cas9 and Cas12a nucleases for targeted mutagenesis in maize. *Plant Biotechnol. J.* **17**, 362–372 (2019).
27. B. P. Kleinstiver, A. A. Sousa, R. T. Walton, Y. E. Tak, J. Y. Hsu, K. Clement, M. M. Welch, J. E. Horng, J. Malagon-Lopez, I. Scarfò, M. V. Maus, L. Pinello, M. J. Aryee, J. K. Joung, Engineered CRISPR–Cas12a variants with increased activities and improved targeting ranges for gene, epigenetic and base editing. *Nat. Biotechnol.* **37**, 276–282 (2019).
28. L. Oesinghaus, F. C. Simmel, Switching the activity of Cas12a using guide RNA strand displacement circuits. *Nat. Commun.* **10**, 2092 (2019).
29. H. R. Kempton, L. E. Goudy, K. S. Love, L. S. Qi, Multiple input sensing and signal integration using a split Cas12a System. *Mol. Cell* **78**, 184–191.e3 (2020).
30. B. Zetsche, S. E. Volz, F. Zhang, A split-Cas9 architecture for inducible genome editing and transcription modulation. *Nat. Biotechnol.* **33**, 139–142 (2015).
31. J. Yin, L. Yang, L. Mou, K. Dong, J. Jiang, S. Xue, Y. Xu, X. Wang, Y. Lu, H. Ye, A green tea-triggered genetic control system for treating diabetes in mice and monkeys. *Sci. Transl. Med.* **11**, eaav8826 (2019).
32. J. Cai, S. Huang, Y. Yi, S. Bao, Ultrasound microbubble-mediated CRISPR/Cas9 knockout of C-erbB-2 in HEC-1A cells. *J. Int. Med. Res.* **47**, 2199–2206 (2019).
33. F. Richter, I. Fonfara, B. Bouazza, C. H. Schumacher, M. Bratovic, E. Charpentier, A. Moglich, Engineering of temperature- and light-switchable Cas9 variants. *Nucleic Acids Res.* **44**, 10003–10014 (2016).
34. Y. Nihongaki, Y. Furuhata, T. Otabe, S. Hasegawa, K. Yoshimoto, M. Sato, CRISPR-Cas9-based photoactivatable transcription systems to induce neuronal differentiation. *Nat. Methods* **14**, 963–966 (2017).
35. L. R. Polstein, C. A. Gersbach, A light-inducible CRISPR-Cas9 system for control of endogenous gene activation. *Nat. Chem. Biol.* **11**, 198–200 (2015).
36. J. Shao, M. Wang, G. Yu, S. Zhu, Y. Yu, B. C. Heng, J. Wu, H. Ye, Synthetic far-red light-mediated CRISPR-dCas9 device for inducing functional neuronal differentiation. *Proc. Natl. Acad. Sci.* **115**, E6722–E6730 (2018).
37. Y. Yu, X. Wu, N. Guan, J. Shao, H. Ye, Engineering a far-red light–activated split-Cas9 system for remote-controlled genome editing of internal organs and tumors. *Sci. Adv.* **6**, eabb1777 (2020).
38. Y. Liu, J. Han, Z. Chen, H. Wu, H. Dong, G. Nie, Engineering cell signaling using tunable CRISPR-Cpf1-based transcription factors. *Nat. Commun.* **8**, 2095 (2017).
39. F. E. Marquard, M. Jucker, PI3K/AKT/mTOR signaling as a molecular target in head and neck cancer. *Biochem. Pharmacol.* **172**, 113729 (2020).
40. X. Wang, X. Chen, Y. Yang, Spatiotemporal control of gene expression by a light-switchable transgene system. *Nat. Methods* **9**, 266–269 (2012).
41. E. J. Olson, J. J. Tabor, Optogenetic characterization methods overcome key challenges in synthetic and systems biology. *Nat. Chem. Biol.* **10**, 502–511 (2014).
42. H. Ye, M. Fussenegger, Optogenetic medicine: Synthetic therapeutic solutions precision-guided by light. *Cold Spring Harb. Perspect. Med.* **9**, a034371 (2019).
43. Y. Nihongaki, T. Otabe, Y. Ueda, M. Sato, A split CRISPR-Cpf1 platform for inducible genome editing and gene activation. *Nat. Chem. Biol.* **15**, 882–888 (2019).
44. M. Mansouri, T. Strittmatter, M. Fussenegger, Light-controlled mammalian cells and their therapeutic applications in synthetic biology. *Adv. Sci.* **6**, 1800952 (2019).
45. J. Shao, S. Xue, G. Yu, Y. Yu, X. Yang, Y. Bai, S. Zhu, L. Yang, J. Yin, Y. Wang, S. Liao, S. Guo, M. Xie, M. Fussenegger, H. Ye, Smartphone-controlled optogenetically engineered cells enable semiautomatic glucose homeostasis in diabetic mice. *Sci. Transl. Med.* **9**, eaal2298 (2017).
46. J. Wu, M. Wang, X. Yang, C. Yi, J. Jiang, Y. Yu, H. Ye, A non-invasive far-red light-induced split-Cre recombinase system for controllable genome engineering in mice. *Nat. Commun.* **11**, 3708 (2020).
47. M. H. Ryu, M. Gomelsky, Near-infrared light responsive synthetic c-di-GMP module for optogenetic applications. *ACS Synth Biol.* **3**, 802–810 (2014).
48. N. Tschowri, M. A. Schumacher, S. Schlimpert, N. B. Chinnam, K. C. Findlay, R. G. Brennan, M. J. Buttner, Tetrameric c-di-GMP mediates effective transcription factor dimerization to control Streptomyces development. *Cell* **158**, 1136–1147 (2014).
49. X. Zhang, W. Wang, L. Shan, L. Han, S. Ma, Y. Zhang, B. Hao, Y. Lin, Z. Rong, Gene activation in human cells using CRISPR/Cpf1-p300 and CRISPR/Cpf1-SunTag systems. *Protein Cell* **9**, 380–383 (2018).
50. A. Chavez, M. Tuttle, B. W. Pruitt, B. Ewen-Campen, R. Chari, D. Ter-Ovanesyan, S. J. Haque, R. J. Cecchi, E. J. K. Kowal, J. Buchthal, B. E. Housden, N. Perrimon, J. J. Collins, G. Church, Comparison of Cas9 activators in multiple species. *Nat. Methods* **13**, 563–567 (2016).
51. S. Bin Moon, J. M. Lee, J. G. Kang, N. E. Lee, D. I. Ha, D. Y. Kim, S. H. Kim, K. Yoo, D. Kim, J. H. Ko, Y. S. Kim, Highly efficient genome editing by CRISPR-Cpf1 using CRISPR RNA with a uridinylate-rich 3′-overhang. *Nat. Commun.* **9**, 3651 (2018).
52. M. E. Tanenbaum, L. A. Gilbert, L. S. Qi, J. S. Weissman, R. D. Vale, A protein-tagging system for signal amplification in gene expression and fluorescence imaging. *Cell* **159**, 635–646 (2014).
53. K. Müller, R. Engesser, S. Metzger, S. Schulz, M. M. Kämpf, M. Busacker, T. Steinberg, P. Tomakidi, M. Ehrbar, F. Nagy, J. Timmer, M. D. Zubriggen, W. Weber, A red/far-red light-responsive bi-stable toggle switch to control gene expression in mammalian cells. *Nucleic Acids Res.* **41**, e77 (2013).
54. S. T. Yen, K. A. Trimmer, N. Aboul-Fettouh, R. D. Mullen, J. C. Culver, M. E. Dickinson, R. R. Behringer, G. T. Eisenhoffer, CreLite: An optogenetically controlled Cre/loxP system using red light. *Dev. Dyn.* **249**, 1394–1403 (2020).
55. A. A. Kaberniuk, A. A. Shemetov, V. V. Verkhusha, A bacterial phytochrome-based optogenetic system controllable with near-infrared light. *Nat. Methods* **13**, 591–597 (2016).
56. T. A. Redchuk, E. S. Omelina, K. G. Chernov, V. V. Verkhusha, Near-infrared optogenetic pair for protein regulation and spectral multiplexing. *Nat. Chem. Biol.* **13**, 633–639 (2017).
57. A. A. Kaberniuk, M. Baloban, M. V. Monakhov, D. M. Shcherbakova, V. V. Verkhusha, Single-component near-infrared optogenetic systems for gene transcription regulation. *Nat. Commun.* **12**, 3859 (2021).
58. M. Tabebordbar, K. A. Lagerborg, A. Stanton, E. M. King, S. Ye, L. Tellez, A. Krunnfusz, S. Tavakoli, J. J. Widrick, K. A. Messemer, E. C. Troiano, B. Moghadaszadeh, B. L. Peacker, K. A. Leacock, N. Horwitz, A. H. Beggs, A. J. Wagers, P. C. Sabeti, Directed evolution of a family of AAV capsid variants enabling potent muscle-directed gene delivery across species. *Cell* **184**, 4919–4938.e22 (2021).
59. P. Gee, M. S. Y. Lung, Y. Okuzaki, N. Sasakawa, T. Iguchi, Y. Makita, H. Hozumi, Y. Miura, L. F. Yang, M. Iwasaki, X. H. Wang, M. A. Waller, N. Shirai, Y. O. Abe, Y. Fujita, K. Watanabe, A. Kagita, K. A. Iwabuchi, M. Yasuda, H. Xu, T. Noda, J. Komano, H. Sakurai, N. Inukai, A. Hotta, Extracellular nanovesicles for packaging of CRISPR-Cas9 protein and sgRNA to induce therapeutic exon skipping. *Nat. Commun.* **11**, 1334 (2020).
60. S. Kannan, H. Altae-Tran, X. Jin, V. J. Madigan, R. Oshiro, K. S. Makarova, E. V. Koonin, F. Zhang, Compact RNA editors with small Cas13 proteins. *Nat. Biotechnol.* 10.1038/s41587-021-01030-2 , (2021).
61. D. Y. Kim, J. M. Lee, S. B. Moon, H. J. Chin, S. Park, Y. Lim, D. Kim, T. Koo, J.-H. Ko, Y.-S. Kim, Efficient CRISPR editing with a hypercompact Cas12f1 and engineered guide RNAs delivered by adeno-associated virus. *Nat. Biotechnol.* 10.1038/s41587-021-01009-z , (2021).
62. E. K. Brinkman, A. N. Kousholt, T. Harmsen, C. Leemans, T. Chen, J. Jonkers, B. van Steensel, Easy quantification of template-directed CRISPR/Cas9 editing. *Nucleic Acids Res.* **46**, e58 (2018).

Acknowledgments: We are grateful to all the laboratory members for cooperation in this study, especially Y. Yu and X. Wu for guidance with T7E1 and TIED assays. **Funding:** This work was financially supported by grants from the National Key R&D Program of China (nos. 2019YFA0904500 and 2019YFA0110802), the National Natural Science Foundation of China (NSFC; nos. 32171414, 31971346, 31861143016, and no.31870861), the Science and Technology Commission of the Shanghai Municipality (no. 18JC1411000), and the Fundamental Research Funds for the Central Universities. This work was also partially supported by the Natural Science Foundation of Shanghai (grant no. 18ZR1436000) to F.C. We also thank the ECNU Multifunctional Platform for Innovation (011) for supporting the mice experiments, and the Instruments Sharing Platform of the School of Life Sciences, East China Normal University. We also thank Addgene for providing the necessary related plasmids.
Author contributions: H.Y. conceived the project. H.Y., X.W., K.D., and M.W. designed the project. X.W., K.D., Y.Z., F.C., and D.K. performed the experimental work. H.Y., X.W., J.Y., and M.W. analyzed the results and wrote the manuscript. All authors edited and approved the manuscript. **Competing interests:** The authors declare that they have no competing interests. **Data and materials availability:** All data needed to evaluate the conclusions in the paper are present in the paper and/or the Supplementary Materials.

Submitted 24 February 2021
Accepted 22 October 2021
Published 10 December 2021
10.1126/sciadv.abh2358

Downloaded from https://www.science.org at Shanghai Normal University on December 16, 2021

ScienceAdvances

A far-red light–inducible CRISPR-Cas12a platform for remote-controlled genome editing and gene activation

Xinyi WangKaili DongDeqiang KongYang ZhouJianli YinFengfeng CaiMeiyan WangHaifeng Ye

Sci. Adv., 7 (50), eabh2358. • DOI: 10.1126/sciadv.abh2358

View the article online
https://www.science.org/doi/10.1126/sciadv.abh2358
Permissions
https://www.science.org/help/reprints-and-permissions

Downloaded from https://www.science.org at Shanghai Normal University on December 16, 2021

Use of think article is subject to the Terms of service

Science Advances (ISSN) is published by the American Association for the Advancement of Science. 1200 New York Avenue NW, Washington, DC 20005. The title *Science Advances* is a registered trademark of AAAS.
Copyright © 2021 The Authors, some rights reserved; exclusive licensee American Association for the Advancement of Science. No claim to original U.S. Government Works. Distributed under a Creative Commons Attribution NonCommercial License 4.0 (CC BY-NC).